Folate Activation and Catalysis in Methylenetetrahydrofolate Reductase from *Escherichia coli*: Roles for Aspartate 120 and Glutamate 28[†]

Elizabeth E. Trimmer,[‡] David P. Ballou, Martha L. Ludwig, and Rowena G. Matthews*

Department of Biological Chemistry and Biophysics Research Division, The University of Michigan, Ann Arbor, Michigan 48109-1055

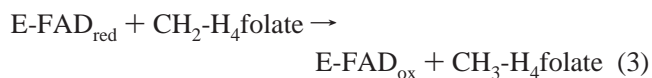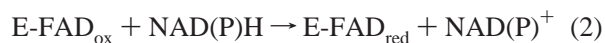*Received December 8, 2000; Revised Manuscript Received March 20, 2001*

ABSTRACT: The flavoprotein *Escherichia coli* methylenetetrahydrofolate reductase (MTHFR) catalyzes the reduction of 5,10-methylenetetrahydrofolate (CH_2-H_4folate) to 5-methyltetrahydrofolate (CH_3-H_4folate). The X-ray crystal structure of the enzyme has revealed the amino acids at the flavin active site that are likely to be relevant to catalysis. Here, we have focused on two conserved residues, Asp 120 and Glu 28. The presence of an acidic residue (Asp 120) near the N1−C2═O position of the flavin distinguishes MTHFR from all other known flavin oxidoreductases and suggests an important function for this residue in modulating the flavin reactivity. Modeling of the CH_3-H_4folate product into the enzyme active site also suggests roles for Asp 120 in binding of folate and in electrostatic stabilization of the putative 5-iminium cation intermediate during catalysis. In the NADH-menadione oxidoreductase assay and in the isolated reductive half-reaction, the Asp120Asn mutant enzyme is reduced by NADH 30% more rapidly than the wild-type enzyme, which is consistent with a measured increase in the flavin midpoint potential. Compared to the wild-type enzyme, the mutant showed 150-fold decreased activity in the physiological NADH-CH_2-H_4folate oxidoreductase reaction and in the oxidative half-reaction involving CH_2-H_4folate, but the apparent K_d for CH_2-H_4folate was relatively unchanged. Our results support a role for Asp 120 in catalysis of folate reduction and perhaps in stabilization of the 5-iminium cation. By analogy to thymidylate synthase, which also uses CH_2-H_4folate as a substrate, Glu 28 may serve directly or via water as a general acid catalyst to aid in 5-iminium cation formation. Consistent with this role, the Glu28Gln mutant was unable to catalyze the reduction of CH_2-H_4folate and was inactive in the physiological oxidoreductase reaction. The mutant enzyme was able to bind CH_3-H_4folate, but reduction of the FAD cofactor was not observed. In the NADH-menadione oxidoreductase assay, the mutant demonstrated a 240-fold decrease in activity.

Methylenetetrahydrofolate reductase (MTHFR)[1] catalyzes the reduction of 5,10-methylenetetrahydrofolate (CH_2-H_4-folate) to 5-methyltetrahydrofolate (CH_3-H_4folate) using flavin adenine dinucleotide (FAD) as coenzyme, as shown in eq 1.

$$CH_2\text{-}H_4\text{folate} + NAD(P)H + H^+ \rightarrow$$
$$CH_3\text{-}H_4\text{folate} + NAD(P)^+ \quad (1)$$
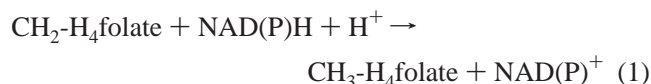
Rapid-reaction kinetic studies described in the preceding paper in this issue (*1*) have established that *Escherichia coli*

MTHFR catalyzes the individual half-reactions constituting this reaction (shown in eqs 2 and 3) at rates consistent with the observed rate of overall turnover.

$$E\text{-}FAD_{ox} + NAD(P)H \rightarrow E\text{-}FAD_{red} + NAD(P)^+ \quad (2)$$

$$E\text{-}FAD_{red} + CH_2\text{-}H_4\text{folate} \rightarrow$$
$$E\text{-}FAD_{ox} + CH_3\text{-}H_4\text{folate} \quad (3)$$

The enzyme employs a ping-pong Bi−Bi mechanism in which $NAD(P)^+$ release precedes the binding of CH_2-H_4-folate. Similar results have been reported for the porcine enzyme (*2, 3*).

Previous studies with porcine MTHFR have investigated the stereochemistry and mechanism of the NAD(P)H-CH_2-H_4folate oxidoreductase reaction. In the reductive half-reaction, NAD(P)H binds at the *si* face of the FAD and the 4S-hydrogen of NAD(P)H is transferred as a hydride to N5 of the FAD cofactor (*4*). $NAD(P)^+$ then dissociates from the enzyme. In the oxidative half-reaction (Scheme 1), CH_2-H_4-folate also binds at the *si* face of the reduced FAD (*5*), consistent with the ping-pong Bi−Bi mechanism. Protonation of N10 is proposed to lead to opening of the five-membered imidazolidine ring of CH_2-H_4folate and to the generation of
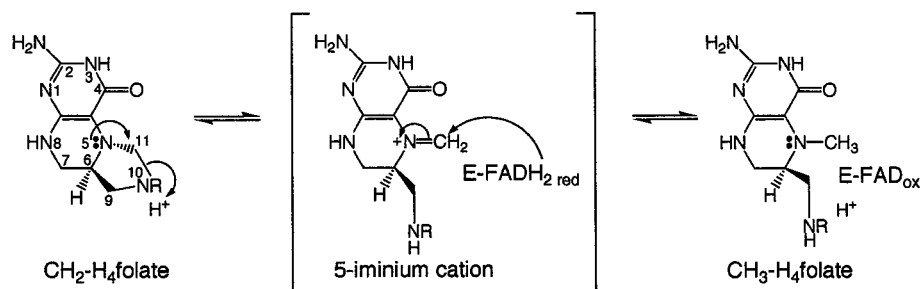
Scheme 1: Proposed Mechanism for Oxidative Half-Reaction

a 5-iminium cation. Transfer of a hydride from N5 of the reduced FAD to the exocyclic methylene group (C11) yields the product CH_3-H_4folate (*5*).

The roles of specific amino acid residues in the enzymatic mechanism of MTHFR are currently unknown. The X-ray structure of *E. coli* MTHFR has been determined (*6*), and it has identified several conserved residues near the flavin that may participate in substrate binding and/or catalysis. In contrast to all other known flavin oxidoreductases, MTHFR was found to have a completely conserved acidic residue (Asp 120) near the N1−C2=O position of the flavin. A basic residue or a positive helix dipole resides at this location in the other flavin oxidoreductases, where the positive charge aids in stabilization of the anionic form of the reduced flavin hydroquinone (Figure 1, structure B) (*7, 8*). The pK_a of Asp 120 in MTHFR is not known; however, we presume that in the reduced state of the enzyme, electrostatic repulsion between a negatively charged aspartate residue and an anionic hydroquinone would favor formation of the neutral flavin hydroquinone (Figure 1, structure C). To test the influence of Asp 120 on the redox properties of the enzyme-bound FAD, we have substituted the neutral asparagine for Asp 120 in *E. coli* MTHFR.

The least understood features of the MTHFR enzyme reaction are those involving the folate substrate. CH_2-H_4-folate is an aminal, the nitrogen analogue of an acetal, and the mechanism by which it undergoes reduction by reduced flavin is of interest. It has been proposed that the first step is an acid-catalyzed opening of the folate ring to form the more reactive 5-iminium cation (Scheme 1). Studies of the nonenzymatic condensation of formaldehyde with H_4folate to form CH_2-H_4folate provide evidence that a 5-iminium cation is an intermediate in that reaction (*9*). Moreover, parallels can be drawn between the folate binding and activation mechanisms of MTHFR and the structurally unrelated enzyme thymidylate synthase (*10*), which utilizes CH_2-H_4folate in the reductive methylation of dUMP to dTMP. In the thymidylate synthase reaction, CH_2-H_4folate, activated by conversion to the 5-iminium cation, undergoes nucleophilic attack by C5 of dUMP to form a ternary covalent intermediate complex. Breakdown of this covalent complex followed by hydride transfer then yields the products dTMP and H_2folate (*11*). Structural evidence for formation of the 5-iminum folate cation has been obtained in thymidylate synthase; a 5-OHCH$_2$-H$_4$folate species, the product of the reaction of a 5-iminium cation with water, was directly observed by X-ray crystallography (*12*).

Figure 2 shows a model of the CH_3-H_4folate product positioned in the proposed folate binding site of *E. coli*

MTHFR (*6*). The modeling started with 5-formyltetrahydrofolate (folinic acid), obtained from the structure of a complex with *E. coli* dihydrofolate reductase (PDB filename 1JOL) (*13*). We retained the pterin ring conformation observed in that study, removed the oxygen of the formyl group, and repositioned the *p*-aminobenzoate (*p*ABA) ring by rotation about the C6−C9, C9−N10, and N10−*p*ABA bonds. In our model, the pterin ring is stacked against the *si* face of the FAD and the C11 methyl group is positioned for transfer of a hydride to N5 of the FAD. Two invariant active site residues, Asp 120 and Gln 183, can form hydrogen bonds with pterin atoms, and the invariant Glu 28 is near N10.

The position of Asp 120 within hydrogen bonding distance of the folate pyrimidine ring suggests two possible roles for this residue in folate binding and catalysis. First, hydrogen bonding between the carboxylate of Asp 120 and the N3 and/or 2-amino groups of the pyrimidine ring (Figure 2) may facilitate binding of CH_2-H_4folate. Structural studies of *E. coli* thymidylate synthase have revealed that a completely conserved aspartate residue (Asp 169) also hydrogen bonds to N3 and, via a water molecule, to the 2-amino group of CH_2-H_4folate (*10, 14*). Moreover, hydrogen-bonding interactions between an aspartate and the pterin ring have been observed in the X-ray structures of the folate-dependent enzymes dihydrofolate reductase (*15*), dihydropteroate synthase (*16, 17*), and methylenetetrahydrofolate dehydrogenase/cyclohydrolase (*18*), suggesting common involvement of an aspartate in folate binding and/or catalysis.

We propose that a second role for Asp 120 in MTHFR is to promote formation and/or stabilization of the putative 5-iminium cation folate intermediate. A negatively charged aspartate may provide favorable electrostatic interactions with the short-lived iminium cation species. An asparagine at position 120 of *E. coli* MTHFR would alter both the hydrogen bonding interactions with the pterin ring and the electrostatics of the active site. To test the influence of Asp 120 on folate binding and catalysis, we prepared the Asp120Asn mutant enzyme.

In the oxidative half-reaction of MTHFR, protonation of N10 by a general acid catalyst on the enzyme would enhance its leaving-group ability and, thereby, facilitate opening of the imidazolidine ring to generate the 5-iminium cation. Structural data have revealed a conserved glutamate (Glu 60) at the active site of *E. coli* thymidylate synthase (*10, 19*). It has been proposed that this glutamate, via a network of water molecules, may be a general acid catalyst involved in protonating N10, the initial step in CH_2-H_4folate activation (*10, 20*). In our model of CH_3-H_4folate bound in the active site of *E. coli* MTHFR (Figure 2), Glu 28 is positioned near
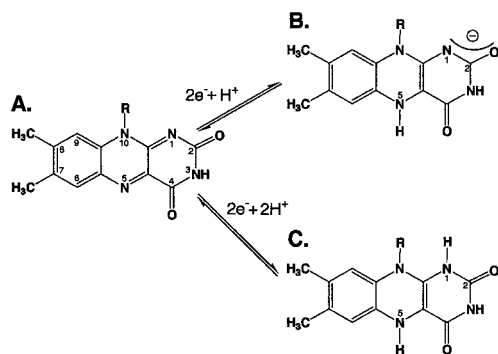
FIGURE 1: Possible structures of oxidized and reduced flavin. (A) Oxidized flavin. (B) Reduced anionic hydroquinone; negative charge resides at the N1−C2=O position. (C) Reduced neutral hydroquinone; N1 is protonated. R refers to ribityl phosphate (FMN) or to ribityl phosphate adenylate (FAD). The pK for ionization of the neutral hydroquinone in solution is 6.7 (*50*).
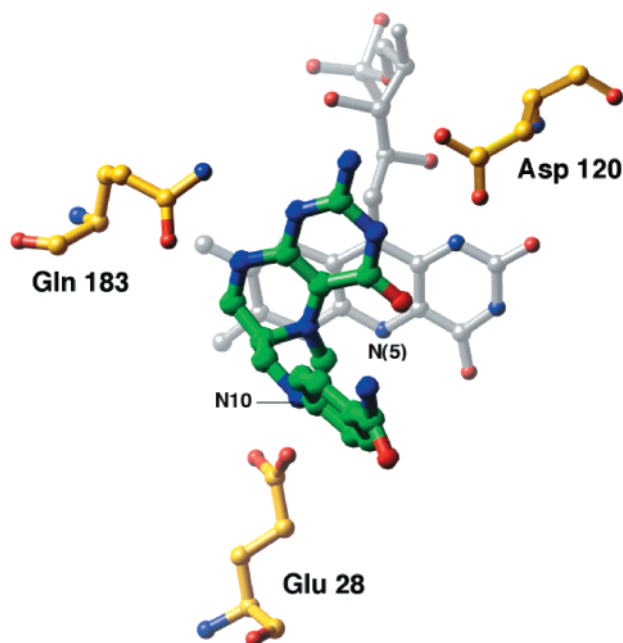

FIGURE 2: Model of CH$_3$-H$_4$folate bound in the active site of *E. coli* methylenetetrahydrofolate reductase. The CH$_3$-H$_4$folate product was generated from 5-formyltetrahydrofolate (folinic acid) (*13*) by removal of the oxygen of the formyl group and repositioning of the *p*ABA ring by rotation of the C6−C9, C9−N10, and N10−*p*ABA bonds. Conserved residues, aspartate 120, glutamate 28, and glutamine 183, of MTHFR are shown.

N10 and the C11 methyl group is close to the N5 of the FAD, situated for hydride transfer. We propose that Glu 28 in MTHFR may serve directly or via water as a general acid catalyst for protonation of N10. To explore the role of Glu 28 in folate activation and catalysis, we have replaced Glu 28 with glutamine.

In this paper, we characterize the MTHFR mutant enzymes Asp120Asn and Glu28Gln. We have determined kinetic parameters for the mutants in each of the three oxidoreductase reactions catalyzed by MTHFR and in the individual half-reactions constituting these reactions by steady-state and stopped-flow kinetic methods. In support of our model for folate binding, we find that both mutations have profound effects on the reaction with folate. Our results underscore the important roles of aspartate and glutamate residues in folate activation and catalysis.

EXPERIMENTAL PROCEDURES

Materials. Robert Blumenthal provided the pGP1-2 plasmid (*21*). Anthraquinone 1-sulfonate was a gift from Vincent Massey. Restriction enzymes were purchased from New England Biolabs. All DNA primers were synthesized at the University of Michigan DNA Synthesis Core Facility. All other materials were as described (*1*).

Methods. All experiments were performed at 25 °C in 50 mM potassium phosphate (pH 7.2) containing 0.3 mM EDTA and 10% glycerol (protein buffer). UV−vis absorption spectra were recorded with a Shimadzu UV2501PC double-beam spectrophotometer or a Hewlett-Packard 8453 diode array spectrophotometer. Rapid-reaction studies were carried out with a Hi-Tech Scientific SF-61 stopped-flow spectrophotometer. Samples for all stopped-flow experiments contained 200 μM protocatechuate (PCA) and ~0.1 units mL^{-1} protocatechuate dioxygenase (PCD) as an oxygen-scavenging system (*22*). All methods were as described in the preceding paper in this issue (*1*) unless otherwise specified below.

Construction of Asp120Asn and Glu28Gln Mutant Plasmids. The starting point for the construction of the Asp120Asn and Glu28Gln mutant plasmids was the pCAS-30 plasmid, a derivative of pET-23b (Novagen, Milwaukee, WI), which contains the *E. coli* MTHFR coding sequence juxtaposed to a C-terminal histidine tag under control of the T7 RNA polymerase promoter (*23*). The mutant plasmids were made by using a PCR-based primer overlap extension method previously described (*23*, *24*). With this method, a total of four PCR primers and two rounds of PCR reactions are needed to produce each mutation. The Asp120Asn mutation was created using the primers DN2* (5′-CTTCCCGGC-GGCAG<u>G</u>TTGCCACGCAGCGCG-3′) and DN3 (5′-GGC-GCTGC<u>G</u>TGGC<u>AAC</u>CTGCCGCCGGGAAG-3′), while the Glu28Gln mutation was created using primers EQ2* (5′-CGCGGCGGGAAAAA<u>T</u>TGGAACGAAACGTTA-3′) and EQ3 (5′-TAACGTTTCGTTC<u>C</u>A<u>A</u>TTTTTCCCGCCGCG-3′). For both mutations, Primers P1 (5′-gaccacaacggtttccct-tctagagtcg-3′) and P4* (5′-GCTTAAAATCTTCACCATATC-CATGGCAAT-3′) were used to synthesize the outside flanking regions containing the *Xba*I and *Nco*I restriction enzyme sites. The asterisks denote sequences corresponding to the coding strand of the *E. coli* MTHFR gene. Sequences contained within the coding region of the gene are shown in uppercase, while those from noncoding regions are in lowercase; underlined sequences indicate changes made to introduce the Asp120Asn or Glu28Gln mutations. The Asp120Asn mutation generated a *Bsp*MI restriction site; the Glu28Gln mutation generated a *Tsp*509I site. The Asp120Asn and Glu28Gln mutant plasmids were constructed by the same procedure. For each mutation, plasmid pCAS-30 (*23*) was used as the template for the first round of PCR reactions, whereas the second round of PCR reactions used the amplified products from the first round as template. The resultant PCR product was digested with *Xba*I and *Nco*I enzymes to generate an 806 bp fragment. This fragment was then ligated into a 3664 bp *Xba*I−*Nco*I fragment of pCAS-30 to generate a 4470 bp expression plasmid. The plasmid containing the Asp120Asn mutation was designated pEET1.8, while that containing the Glu28Gln mutation was designated pEET3.10. The sequences of the mutant plasmids were confirmed by restriction enzyme analyses and by DNA

sequencing at the University of Michigan Sequencing Core Facility.

Expression and Purification of Asp120Asn and Glu28Gln Mutants. To eliminate wild-type contamination of the Asp120Asn and Glu28Gln mutants, it was desirable to express the mutant plasmids in *E. coli* strain AB1909 (*metF arg lac*) (*25*). Strain AB1909 contains an uncharacterized mutation in the MTHFR (*metF*) gene, which leads to inactivity of the enzyme and methionine auxotrophy (*25*). Because AB1909 lacks the ability to express T7 RNA polymerase, which is necessary for production of the mutant proteins, the strain was first transformed with plasmid pGP1-2 (*21*). This plasmid contains the gene for T7 RNA polymerase under control of the λp_L promoter that is repressed by a temperature-sensitive repressor (*cI857*); in addition, it contains the gene encoding resistance to kanamycin. Thus, at 30 °C, the *cI857* repressor inhibits transcription of T7 RNA polymerase; at 42 °C, the repressor is inactivated, allowing expression of the polymerase.

Transformation of *E. coli* AB1909/pGP1-2 with the Asp120Asn mutant plasmid (pEET1.8) generated the strain EET-10, whereas transformation with the Glu28Gln plasmid (pEET3.10) generated strain EET-12. For production of the mutant MTHFRs, 1 L of LB medium containing 60 μg/mL ampicillin, 60 μg/mL kanamycin, and 10 μM riboflavin was inoculated to an OD_{600} of ~0.05 with strain EET-10 or EET-12. The cells were allowed to grow at 30 °C for ~3 h until they reached an OD_{600} of 1.0. Protein expression was induced by placing the cultures in a 42 °C water bath for 30 min. After heat induction, the cells were grown at 37 °C until they reached stationary phase (OD_{600} of ~5), after about 4 h, and then they were harvested. The cell pellets were frozen in liquid N_2 and stored at −80 °C prior to protein purification. The histidine-tagged Asp120Asn and Glu28Gln mutant proteins were purified by the procedure described (*1*) with the following modification. To improve the yield, the cells were sonicated in a low salt buffer (20 mM sodium phosphate, pH 7.4, 10 mM imidazole, and 10% glycerol). Following centifugation, NaCl was added to the supernatant to a final concentration of 0.5 M. Using this procedure, 15 mg of purified mutant protein were obtained from 1 L of cell culture. High levels of expression of the histidine-tagged mutant proteins and growth in LB medium containing methionine, which strongly represses expression from the wild-type *metF* promoter, ensure that significant oligomerization of mutant and wild-type protein does not occur.

Midpoint Potential Determination. The midpoint potentials for the Asp120Asn and Glu28Gln enzymes were determined as described for the wild-type enzyme (*1*), but with the following modifications. Anthraquinone 1-sulfonate was used as the redox dye at a concentration of 40 μM. The E_m for the anthraquinone 1-sulfonate redox couple is −218 mV at pH 7.0 (*26*), and at pH 7.2, E_m is calculated to be −230 mV (*27*). Because of significant overlap between the absorbance spectra of oxidized/reduced dye and oxidized/reduced enzyme, a single wavelength could not be used to follow the reduction of dye or enzyme. Instead, for each spectrum, the contributions of the absorbing species (oxidized/reduced dye, oxidized/reduced enzyme) at two wavelengths, 379 nm (λ_{max} for reduced dye) and 447 nm (λ_{max} for oxidized enzyme), were calculated by the following method. The extinction coefficients of each absorbing species at the 379 and 447

nm wavelengths were determined by titrating enzyme in the absence of redox dye and by titrating anthraquinone 1-sulfonate dye in the absence of enzyme using the xanthine/xanthine oxidase method. The values calculated for the extinction coefficients (ϵ) at 379 nm were (E, enzyme; D, Dye; all units in M^{-1} cm^{-1}) D_{ox}, 438; D_{red}, 5844; E_{ox}, 11083; E_{red}, 5233. At 447 nm, the extinction coefficients were (all units in M^{-1} cm^{-1}) D_{ox}, 130; D_{red}, 3202; E_{ox}, 14100; E_{red}, 1543. The application of Beer's law (path length = 1 cm) yielded eq 4.

$$\text{Abs} = \epsilon_{E_{ox}} c_{E_{ox}} + \epsilon_{E_{red}} c_{E_{red}} + \epsilon_{D_{ox}} c_{D_{ox}} + \epsilon_{D_{red}} c_{D_{red}} \quad (4)$$

Employing 20 and 40 μM as the total concentrations of enzyme and dye, respectively, and rearranging, Eq 5

$$\text{Abs} = c_{E_{ox}}(\epsilon_{E_{ox}} - \epsilon_{E_{red}}) + c_{D_{ox}}(\epsilon_{D_{ox}} - \epsilon_{D_{red}}) + $$
$$\epsilon_{E_{red}}(20 \times 10^{-6} \text{ M}) + \epsilon_{D_{red}}(40 \times 10^{-6} \text{ M}) \quad (5)$$

was applied to data collected at wavelengths 379 and 447 nm over the time period of the experiment. Using the program Excel (Microsoft Corporation), the set of two equations and two unknowns was solved for each spectrum, yielding the concentrations of oxidized enzyme and oxidized dye. The corresponding concentrations of reduced enzyme and reduced dye were then computed, and the midpoint potential was determined using the method of Minneart (*28*).

Titration of Enzyme with CH₃-H₄folate. Titrations were performed using anaerobic cuvettes equipped with capillary fittings for gastight Hamilton syringes (*29*). A 1.2 mL solution of 15 μM enzyme was placed in an anaerobic cuvette and deaerated by 10 cycles of alternate evacuation and equilibration with oxygen-free argon. Under anaerobic conditions, the enzyme solution was titrated with aliquots of an anaerobic 3.3 mM solution of (6S)-CH₃-H₄folate. After each addition of (6S)-CH₃-H₄folate (0.5−5 M equiv), an absorbance spectrum between 200 and 800 nm was recorded.
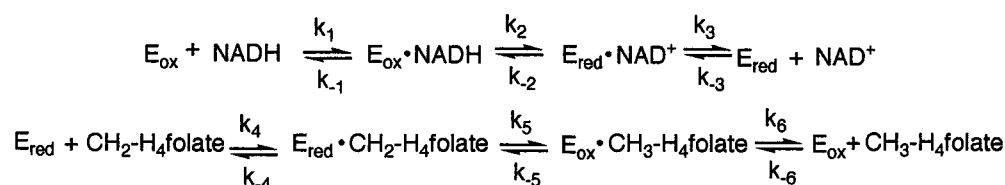
RESULTS

Spectral Properties Are Not Significantly Affected by Mutations Asp120Asn or Glu28Gln. The *E. coli* AB1909 strain containing a mutation in the wild-type MTHFR gene (*25*) was used to produce the Asp120Asn and Glu28Gln mutants. The mutant proteins were purified by the same procedure as wild-type MTHFR. The absorbance spectrum of the Asp120Asn mutant was identical to that of the wild-type enzyme, with a maximum at 447 nm for the enzyme-bound FAD. The maximal absorbance of the Glu28Gln enzyme was shifted slightly to 448.5 nm. The molar extinction coefficients of the two mutants were determined to be 14 300 M^{-1} cm^{-1}, the same as that reported for the wild-type enzyme (*23*). FAD is nonfluorescent when bound to wild-type MTHFR (*6*) or to either of the two mutant enzymes. The similar spectral properties of the mutant and wild-type enzymes suggest that the protein structure has not been perturbed significantly by either mutation. Preliminary X-ray structural data on the Glu28Gln mutant support this view (Guenther, B. D., Garrett, E. G., and Ludwig, M. L. unpublished results).

Enzyme Midpoint Potential Is Raised by Mutations Asp120Asn or Glu28Gln. In flavoproteins, the midpoint

Table 1: Midpoint Potential and Rapid-Reaction Kinetic Constants[a,b]

	Asp120Asn	Glu28Gln	wild-type[c]
midpoint potential (mV)	-210 ± 4	-207 ± 4	-237 ± 4
reductive half-reaction with NADH			
k'_2 (s^{-1})	70 ± 7	0.23 ± 0.04	55 ± 6
K_d for NADH (μM)	12 ± 2	73 ± 7	32 ± 5
oxidative half-reaction with CH$_2$-H$_4$folate			
k'_5 (s^{-1})	0.072 ± 0.008	no reoxidation	10.3 ± 1.0
K_d for CH$_2$-H$_4$folate (μM)	21 ± 3	nd[d]	11 ± 1
reductive half-reaction with CH$_3$-H$_4$folate			
k'_{-5} (s^{-1})	0.062 ± 0.007	binding, no reduction	2.5 ± 0.5
K_d for CH$_3$-H$_4$folate (μM)	22 ± 7	nd	nd

[a] All determinations were at 25 °C in 50 mM potassium phosphate buffer (pH 7.2) containing 0.3 mM EDTA and 10% glycerol. [b] Values of rate constants were the average of two or three experiments. Definition of rate constants are given in Scheme 2. [c] Ref *1*. [d] Not determined.

Scheme 2: Kinetic Mechanism for the NADH-CH$_2$-H$_4$folate Oxidoreductase Reaction

$$E_{ox} + NADH \underset{k_{-1}}{\overset{k_1}{\rightleftharpoons}} E_{ox}{\cdot}NADH \underset{k_{-2}}{\overset{k_2}{\rightleftharpoons}} E_{red}{\cdot}NAD^+ \underset{k_{-3}}{\overset{k_3}{\rightleftharpoons}} E_{red} + NAD^+$$

$$E_{red} + CH_2\text{-}H_4folate \underset{k_{-4}}{\overset{k_4}{\rightleftharpoons}} E_{red}{\cdot}CH_2\text{-}H_4folate \underset{k_{-5}}{\overset{k_5}{\rightleftharpoons}} E_{ox}{\cdot}CH_3\text{-}H_4folate \underset{k_{-6}}{\overset{k_6}{\rightleftharpoons}} E_{ox} + CH_3\text{-}H_4folate$$

potential (E_m) of the bound flavin can be significantly influenced by the protein environment surrounding the flavin. A redox dye method (*30*) described in ref *1* was employed to determine the two-electron midpoint potentials of the Asp120Asn and Glu28Gln mutant enzymes at pH 7.2 and 25 °C. In this method, a redox dye is chosen that has a midpoint potential within ±30 mV from that of the unknown. After preliminary studies indicated that the mutant enzymes were more readily reduced compared to a phenosafranine dye ($E_m = -258$ mV at pH 7.2), anthraquinone 1-sulfonate, a redox dye of higher midpoint potential (-230 mV at pH 7.2) (*27*) was used. For both mutant enzymes, the resulting Nernst plots (data not shown) were linear, except for the points corresponding to less than 10% or more than 90% reduced dye or enzyme. From the linear portions of the plots, the midpoint potentials were determined to be -210 ± 4 and -207 ± 4 mV for the Asp120Asn and Glu28Gln mutants, respectively (Table 1). Experiments employing phenosafranine as redox dye yielded midpoint potential values similar to those determined with anthraquinone 1-sulfonate.

In summary, the measured midpoint potentials of the Asp120Asn and Glu28Gln mutants were 27−30 mV greater than that of the wild-type enzyme [-237 mV (*1*)], consistent with a loss of negative charge near the flavin in both of the mutant enzymes. An average 29 mV increase in the midpoint potential corresponds to a relative thermodynamic stabilization of 1.3 kcal mol^{-1} for the reduced form of the enzyme. Thus, our results predict that the enzyme-bound flavins of the Asp120Asn and Glu28Gln mutants will be more easily reduced, and once reduced, they will be more difficult to reoxidize compared to the wild-type enzyme.

Asp120Asn Mutation Increases the Rate of Reduction by NADH. To obtain a clearer picture of catalysis by the Asp120Asn mutant, the reductive and oxidative half-reactions constituting the three oxidoreductase reactions (Scheme 1 in ref *1*) have been examined in detail. The kinetic rate constants for the NADH−CH$_2$-H$_4$folate oxidoreductase reac-

tion are diagrammed in Scheme 2. Reduction of Asp120Asn mutant enzyme by NADH was studied under anaerobic conditions in a stopped-flow spectrophotometer at pH 7.2 and 25 °C. The reaction was monitored at 450, 550, and 650 nm and fit to biphasic exponential curves. As described for the wild-type enzyme in the previous paper in this issue (*1*), a transient charge-transfer absorbance at 550 and 650 nm was observed for the Asp120Asn enzyme during the course of reduction (data not shown). At NADH concentrations of 10 and 25 μM (after mixing), the phase associated with the rapid increase in absorbance was seen. At higher NADH concentrations, the fast phase occurred within the dead time of the apparatus. The slow phase, however, was clearly apparent and corresponded to the decrease in absorbance at 450 nm. Figure 3 shows the 450 nm traces from a representative experiment. The observed rate constant for reduction showed a hyperbolic dependence on the concentration of NADH (inset). A fit of the data to eq 6 yielded an apparent K_d for NADH of 12 ± 2 μM and a maximum observed rate constant (net rate constant k'_2, according to Scheme 2) of 70 ± 7 s^{-1}, 1.3-fold higher than that for the wild-type enzyme (Table 1). In summary, these results are consistent with more facile reduction of the enzyme-bound flavin of the mutant, predicted from the measured increase in the thermodynamic driving force for reduction (Table 1).

$$k_{obs} = \frac{k_{max}[S]}{K_d + [S]} \qquad (6)$$

Asp120Asn Mutation Significantly Decreases the Rate of Reaction with Folate. On the basis of our modeling studies with CH$_3$-H$_4$folate, we proposed that Asp 120 would participate in folate binding and catalysis. We predicted that the substitution of an asparagine for Asp 120 would impair reaction with the folate substrate. In the physiological oxidoreduction, CH$_2$-H$_4$folate is reduced to CH$_3$-H$_4$folate concomitant with reoxidation of the reduced enzyme (Scheme 2, above). In a stopped-flow spectrophotometer, we have
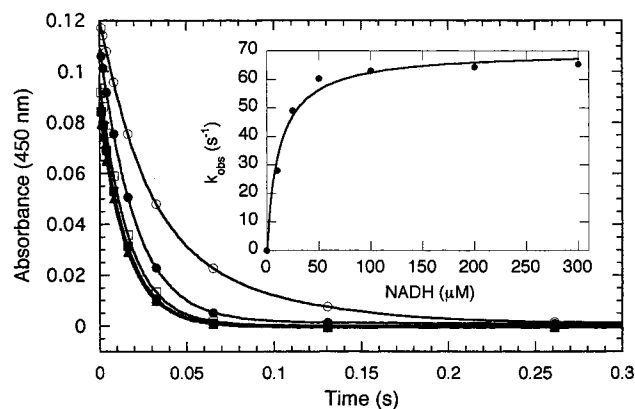
FIGURE 3: Reduction of Asp120Asn enzyme by NADH. Oxidized enzyme, 10 μM, was mixed with solutions of 10 (○), 25 (●), 50 (□), 100 (■), 200 (△), and 300 (▲) μM NADH (concentrations after mixing). Stopped-flow reaction traces, monitored at 450 nm, were fit to two exponential phases. (Inset) Dependence of the observed rate constant for reduction (slow phase) on NADH concentration. The data were fit to eq 6 which yielded an apparent K_d of 12 ± 2 μM for NADH and a k_2' of 70 ± 7 s^{-1}.

examined the reaction of photoreduced Asp120Asn enzyme with CH_2-H_4folate at pH 7.2 and 25 °C. The reoxidation was monitored by measuring the increase in flavin absorbance at 450 nm. Spectra taken after each shot indicated that the flavin was not fully reoxidized at low concentrations of CH_2-H_4folate; full reoxidation was only achieved on adding 200 and 300 μM CH_2-H_4folate (concentrations after mixing). This difficulty in achieving full reoxidation reflects the fact that the reaction proceeds to equilibrium rather than to completion under these conditions. A small, positive free energy change of $+0.09$ kcal mol^{-1} at pH 7.2 corresponding to a -2 mV difference in midpoint potential can be calculated using the respective potentials of the mutant enzyme (-210 mV, Table 1) and of the CH_2-H_4folate/CH_3-H_4folate redox couple at pH 7.2 (-212 mV) (*31*). The 450 nm reaction traces (Figure 4A) were fit well to one exponential phase. This is in contrast to the biphasic reaction traces observed for the wild-type enzyme (see Figure 4 of ref *1*), suggesting the absence of a transient enzyme-folate complex or a change in the rate-limiting step for the mutant. A fit of the data to eq 6 (Figure 4B) resulted in an apparent K_d for CH_2-H_4folate of 21 ± 3 μM, only a 2-fold increase over that observed for the wild-type enzyme. The maximum observed rate constant for oxidation (net rate constant k_5', according to Scheme 2) was 0.072 ± 0.008 s^{-1}, 150-fold lower than the rate constant for the wild-type enzyme. These results indicate that the half-reaction involving the reduction of CH_2-H_4folate has been impaired by the Asp120Asn mutation, but CH_2-H_4folate binding to the enzyme has been relatively unaffected.

As is evident from a small, positive free energy change of $+0.09$ kcal mol^{-1} in the physiological direction, reaction of the Asp120Asn mutant with folate should be reversible. The reduction of the Asp120Asn enzyme by CH_3-H_4folate was investigated in a stopped-flow apparatus (data not shown). A fit of the data to eq 6 yielded an apparent K_d for CH_3-H_4folate of 22 ± 7 μM and a maximum observed rate constant (net rate constant k_{-5}') of 0.062 ± 0.007 s^{-1}, 40-fold lower than that for the wild-type enzyme (Table 1). Taken together, our stopped-flow kinetic data indicate that the Asp120Asn mutation has significantly reduced the ability
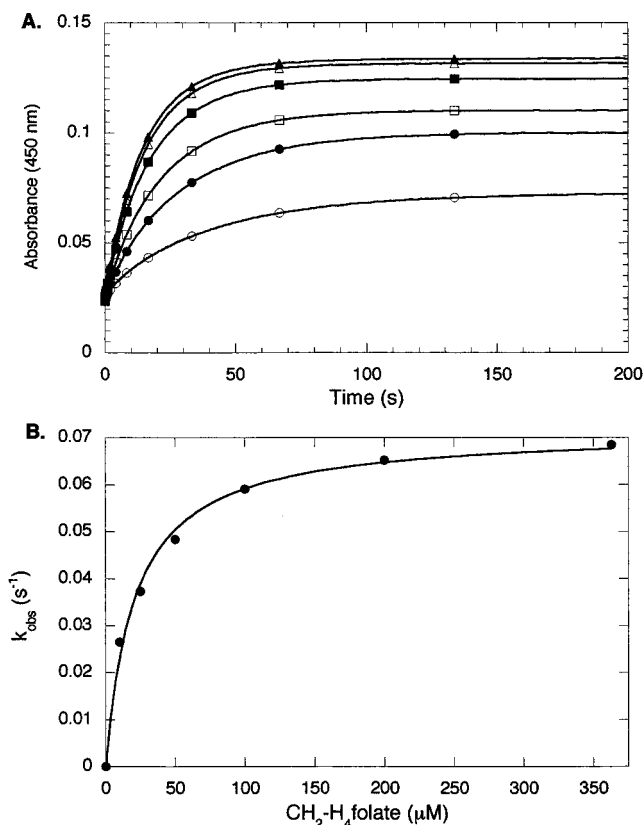

FIGURE 4: Reoxidation of reduced Asp120Asn enzyme by CH_2-H_4folate. (A) Photoreduced enzyme (10 μM) was mixed with solutions of 10 (○), 25 (●), 50 (□), 100 (■), 200 (△), and 300 (▲) μM CH_2-H_4folate (concentrations after mixing). Stopped-flow reaction traces were monitored at 450 nm and fit to one exponential phase. B. Dependence of the observed rate constant on CH_2-H_4-folate concentration. The data were fit to a eq 6 which yielded an apparent K_d of 21 ± 3 μM for CH_2-H_4folate and a k_5' of 0.072 ± 0.008 s^{-1}.

of the enzyme to catalyze folate-dependent reactions in either direction.

Asp120Asn Mutation Significantly Decreases Turnover in the Physiological NADH-CH_2-H_4folate Oxidoreductase Reaction. The physiological oxidoreductase reaction occurs by transfer of reducing equivalents from NADH to the enzyme-bound FAD and then from the reduced FAD to CH_2-H_4folate. From the maximum observed rate constants for the two half-reactions catalyzed by the Asp120Asn mutant, reduction of flavin by NADH (70 s^{-1}) and reoxidation of the flavin by CH_2-H_4folate (0.072 s^{-1}) (Table 1), an expected value of 0.072 s^{-1} can be calculated for the steady-state turnover number of the reaction, assuming a ping-pong Bi—Bi mechanism (*32*).

$$\frac{v}{E_T} = \frac{k_2' k_5'}{k_2' + k_5'} \text{ s}^{-1} = \frac{(70)(0.072)}{(70 + 0.072)} \text{ s}^{-1} = 0.072 \text{ s}^{-1} \quad (7)$$

This analysis shows that, for the Asp120Asn enzyme, the reoxidation of the flavin by CH_2-H_4folate will be substantially more rate limiting in overall turnover than the reductive half-reaction. We predict, therefore, that the diminished rate of folate-linked reoxidation induced by the Asp120Asn mutation will also reduce turnover in the physiological oxidoreduction. To test this prediction, a steady-state analysis of the reaction was carried out under anaerobic conditions in a stopped-

Table 2: Steady-State Kinetic Constants[a,b]

	Asp120Asn	Glu28Gln	wild-type[c]
NADH-CH$_2$-H$_4$folate oxidoreductase assay			
k_{cat} (s^{-1})	0.057 $\pm$ 0.007	<0.0002	10.4 $\pm$ 1
K_m for NADH (μM)	<5.0	nd[d]	20 $\pm$ 4
K_m for CH$_2$-H$_4$folate (μM)	27 $\pm$ 3	nd	0.5 $\pm$ 0.1
CH$_3$-H$_4$folate-menadione oxidoreductase assay			
k_{cat} (s^{-1})	0.087 $\pm$ 0.008	<0.002	3.2 $\pm$ 0.4
K_m for CH$_3$-H$_4$folate (μM)	106 $\pm$ 10	nd	85 $\pm$ 9
NADH-mendione oxidoreductase assay			
k_{cat} (s^{-1})	54 $\pm$ 5	0.20 $\pm$ 0.02	55 $\pm$ 8.3
K_m for NADH (μM)	17 $\pm$ 3	80 $\pm$ 6	66 $\pm$ 16
K_i for NADH (μM)	40 $\pm$ 20	nd	12 $\pm$ 5

[a] Kinetic constants were determined at 25 °C in 50 mM potassium phosphate buffer (pH 7.2) containing 0.3 mM EDTA and 10% glycerol. [b] Values of constants were the average of two to four experiments. [c] Ref *1*. [d] Not determined.

flow spectrophotometer. The K_m for NADH was estimated to be less than 5.0 $\pm$ 1 μM, the K_m for CH$_2$-H$_4$folate was 27 $\pm$ 3 μM, and the maximum turnover number (k_{cat}) was 0.057 $\pm$ 0.007 s^{-1}, 175-fold lower compared to the wild-type enzyme (Table 2). This observed turnover number is in reasonable agreement with the expected value of 0.072 $\pm$ 0.008 s^{-1} calculated above. As predicted from the stopped-flow data, the Asp120Asn mutant has significantly reduced activity in the NADH-CH$_2$-H$_4$folate oxidoreductase assay.

Asp120Asn Mutation Affects Turnover in the Steady-State CH$_3$-H$_4$folate-Menadione and NADH-Menadione Oxidoreductase Assays. Under aerobic conditions, MTHFR catalyzes the CH$_3$-H$_4$folate-menadione (eq 8) and NADH-menadione oxidoreductase (eq 9) reactions (see Scheme 1, parts C and B, respectively, in ref *1*):

$$CH_3\text{-}H_4\text{folate} + \text{menadione} \rightarrow$$
$$CH_2\text{-}H_4\text{folate} + \text{menadiol} \quad (8)$$

$$NADH + \text{menadione} \rightarrow NAD^+ + \text{menadiol} \quad (9)$$
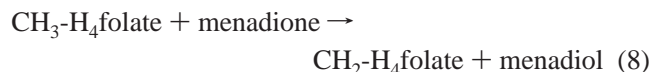
In these reactions, menadione is used as the electron acceptor to reoxidize the reduced FAD. The reaction of reduced Asp120Asn enzyme with menadione at the concentrations used is very fast; the pseudo first-order rate constant (1400 $\pm$ 500 s^{-1}) is similar to that of the wild-type enzyme (data not shown). Thus, in both of these assays, the rate is limited by the respective reductive half-reactions.

The CH$_3$-H$_4$folate-menadione oxidoreductase assay was carried out with the Asp120Asn enzyme in the presence of saturating menadione (140 μM). A fit of the data to the Michaelis–Menten equation yielded a K_m for CH$_3$-H$_4$folate of 106 $\pm$ 10 μM and a k_{cat} of 0.087 $\pm$ 0.008 s^{-1}, a decrease of 36-fold compared to the wild-type enzyme (Table 2). Again, the rate of the limiting folate-dependent reaction has been significantly decreased by the Asp120Asn mutation.

When the NADH-menadione oxidoreductase assay was performed in the presence of saturating menadione, excess substrate inhibition by NADH was observed for the Asp120Asn enzyme. Applying 140 μM as the concentration of menadione (B) and 4 μM as the K_m for menadione (determined in an earlier experiment, data not shown), the data were fit to eq 10 for single substrate inhibition (*33*).

$$\frac{v}{E_T} = \frac{[A][B]k_{cat}}{K_{mB}[A](1 + [A]/K_{iA}) + K_{mA}[B] + [A][B]} \quad (10)$$

The K_{mA} for NADH (A) was calculated to be 17 $\pm$ 3 μM, K_{iA} for NADH (A) was 40 $\pm$ 20 μM, and the k_{cat} was 54 $\pm$ 5 s^{-1} (Table 2). As described in the preceding paper in this issue (*1*), the net rate constant for reduction measured in the stopped-flow apparatus (k'_2) is equivalent to k_{cat} measured in steady-state turnover when $k_3 \gg k_2$, i.e., when NAD$^+$ product release is fast compared to flavin reduction (see Scheme 2). The Asp120Asn mutant is reduced by NADH with an observed rate constant (k'_2) of 70 s^{-1} (Figure 3, Table 1), while the observed rate of turnover in the NADH-menadione oxidoreductase assay is 54 s^{-1} (Table 2), a 20% lower value. These data indicate that, in contrast to the wild-type enzyme, release of NAD$^+$ may be partially rate limiting for the Asp120Asn mutant.

Glu28Gln Mutation Renders the Enzyme Inactive in Reactions with Folate. On the basis of our CH$_3$-H$_4$folate modeling studies and by analogy to thymidylate synthase, we proposed that Glu 28, located near N10 of folate (Figure 2), may serve as a general acid catalyst involved in activating CH$_2$-H$_4$folate. We therefore expected that replacement of Glu 28 with a glutamine would impair both formation of the crucial 5-iminium cation intermediate and the overall reaction with folate, so we examined the reoxidation of photoreduced Glu28Gln enzyme by CH$_2$-H$_4$folate in a stopped-flow spectrophotometer. At concentrations of CH$_2$-H$_4$folate up to 300 μM (after mixing), no increase in flavin absorbance at 450 nm was observed (data not shown). The mutant enzyme was unable to use CH$_2$-H$_4$folate as a substrate and become reoxidized. In a similar manner, the Glu28Gln enzyme was inactive in the NADH-CH$_2$-H$_4$folate oxidoreductase assay, where reducing equivalents must be transferred from NADH to CH$_2$-H$_4$folate (Table 2). To examine folate catalysis in reverse of the physiological direction, the steady-state CH$_3$-H$_4$folate-menadione oxidoreductase assay was performed in the presence of saturating menadione. The mutant had no detectable turnover (k_{cat} < 0.002 s^{-1}) (Table 2).

Although the Glu28Gln enzyme is not reducible by CH$_3$-H$_4$folate, evidence for substrate binding has been obtained by titration. Addition of one equiv of CH$_3$-H$_4$folate to oxidized Glu28Gln enzyme under anaerobic conditions led to a shift in the absorbance spectrum of the enzyme-bound FAD, suggesting the formation of an E$_{ox}$-CH$_3$-H$_4$folate complex (Figure 5A). For comparison, Figure 5B shows reduction of the wild-type enzyme on addition of CH$_3$-H$_4$folate. Taken together, our data demonstrate that the Glu28Gln mutation has substantially reduced the ability of the enzyme
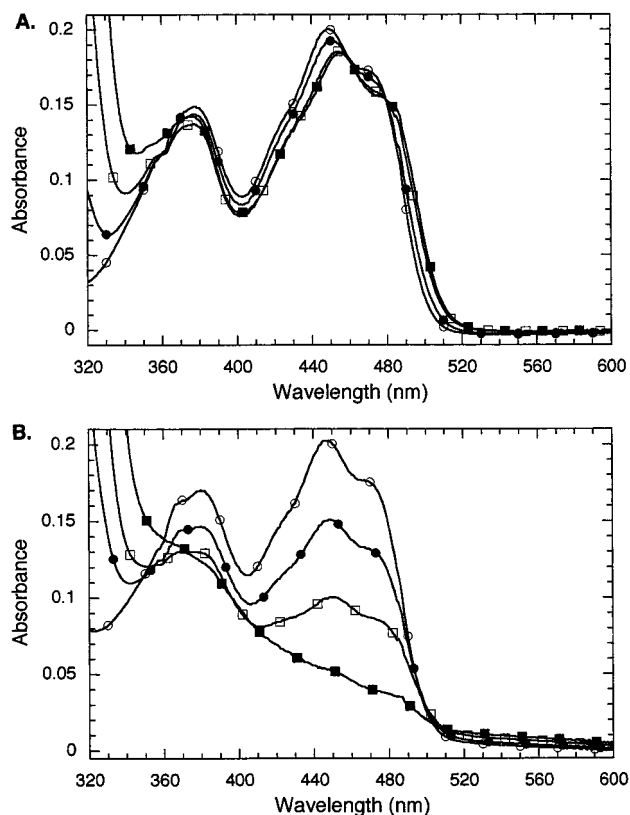
FIGURE 5: Titration of enzyme with CH_3-H_4folate. Oxidized enzyme, 15 μM (18 nmol), was titrated with aliquots of 3.3 mM 6S-CH_3-H_4folate under anaerobic conditions. Spectra correspond to addition of 0 (○), 0.5 (●), 1.0 (□), and 5.0 (■) equiv of 6S-CH_3-H_4folate, respectively. (A) Binding of CH_3-H_4folate to the Glu28Gln enzyme is represented by the observed shift. No reduction of the FAD was observed. (B) Reduction of wild-type enzyme by CH_3-H_4folate.

to catalyze folate-dependent reactions in either direction. These results are consistent with a role for Glu 28 in 5-iminium cation formation, perhaps as a general acid catalyst. Note that the 30 mV increase in midpoint potential observed for the Glu28Gln mutant (Table 1) predicts that the mutant would be more easily reduced than the wild-type enzyme by CH_3-H_4folate. This clearly is not true, suggesting that there is a kinetic/mechanistic impairment of the mutant rather than a redox problem.

Glu28Gln Mutation Also Impairs Reaction with NADH. In a stopped-flow spectrophotometer, the reduction of the Glu28Gln mutant by NADH was monitored at 450 and 650 nm. No change in absorbance was observed at 650 nm, indicating the lack of a flavin-pyridine nucleotide charge-transfer complex. The reaction traces at 450 nm were fit to monophasic exponential curves (Figure 6). The inset shows a plot of the observed rate constants vs the concentration of NADH. The data yielded an apparent K_d for NADH of 73 ± 7 μM, an increase of 2.3-fold compared to the wild-type enzyme. The maximum observed rate constant (net rate constant k_2') was 0.23 ± 0.04 s^{-1}, 240-fold lower than that for the wild-type enzyme (Table 1). Similar results were seen under steady-state conditions in the NADH-menadione oxidoreductase assay, where turnover is limited by NADH reduction. The k_{cat} was determined to be 0.20 ± 0.02 s^{-1} and the K_m for NADH was 80 ± 6 μM, 1.2-fold greater than for the wild-type enzyme (Table 2). Taken together, these results indicate that reduction of the enzyme by NADH has

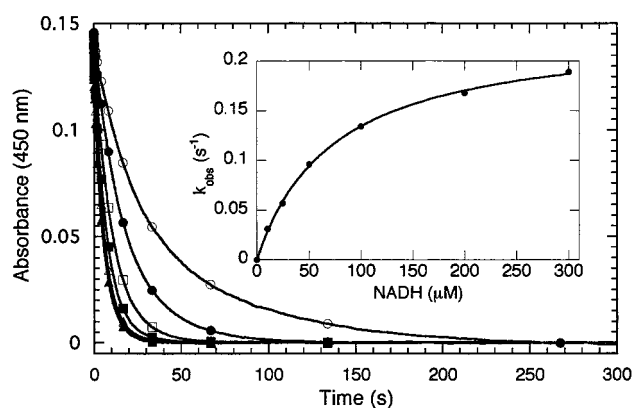FIGURE 6: Reduction of Glu28Gln enzyme by NADH. Oxidized enzyme, 10 μM, was mixed with solutions of 10 (○), 25 (●), 50 (□), 100 (■), 200 (△), and 300 (▲) μM NADH (concentrations after mixing). Stopped-flow reaction traces, monitored at 450 nm, were monophasic. (Inset) Dependence of the observed rate constant for reduction on NADH concentration. The data were fit to a eq 6 which yielded an apparent K_d of 73 ± 7 μM for NADH and a k_2' of 0.23 ± 0.04 s^{-1}.

been significantly impaired by the Glu28Gln mutation, but NADH binding has been only minimally affected.

DISCUSSION

Asp 120 Influences Flavin Reactivity. Flavin oxidoreductases vary in structural motif, substrate specificity, and reaction catalyzed. However, in nearly all the structures examined, a positively charged protein moiety is within 3.5 Å of the N1−C2=O position of the flavin (*8*). The "N1−C2=O protein moiety" can be a fully charged lysine or arginine residue or a partially charged histidine or the positive end of an α helix dipole. There are two possible functional roles for the positive charge at this location (*34*). First, any interaction with the protein that lowers the negative charge density near the flavin cofactor is expected to raise the midpoint potential, making the flavin easier to reduce. Second, upon reduction of the flavin, a positive charge from the protein at the N1−C=O position would likely stabilize preferentially the anionic flavin hydroquinone rather than the neutral hydroquinone (see Figure 1). Studies with anionic flavin analogues have generally supported this view (*35*). Moreover, ^{15}N NMR experiments have shown definitively that in the reduced state, the flavin is bound as the anionic hydroquinone in glucose oxidase (*36*) and *p*-hydroxybenzoate hydroxylase (*37*), enzymes that contain a histidine and a positive helix dipole as the N1−C2=O protein moiety, respectively.

In MTHFR, Asp120 is positioned with one of its oxygens in van der Waals contact (<3.8 Å) with N1−C2=O of the flavin. The presence of a potentially negatively charged residue at this position near the FAD distinguishes MTHFR from all other known flavin oxidoreductases. The protonation state of Asp 120 within MTHFR is not known. However, if the pK_a of the side chain is similar to that in solution (pK_a ≈ 4), the Asp 120 would be ionized as the carboxylate. In the present work, we have replaced Asp 120 with a neutral asparagine residue in order to investigate the influence of charge on the redox properties of the enzyme-bound FAD. As expected for a loss of negative charge near the flavin, the midpoint potential of the Asp120Asn mutant (−210 mV,

Table 1) is higher than that of the wild-type enzyme. The 27 mV increase in potential is very similar in magnitude to the 31 mV decrease observed for a methionine substitution of a lysine (Lys 266) located next to the N1−C2=O flavin position in lactate monooxygenase (*38*). We propose that the N1−C2=O protein moiety of a flavin enzyme can modulate the redox properties of the flavin by directly influencing the protonation state of the reduced flavin hydroquinone. In the case of *E. coli* MTHFR, the presence of a negatively charged aspartate at the N1−C2=O position suggests that the reduced FAD will be bound as the neutral hydroquinone rather than the anion (see Figure 1) so as to avoid unfavorable electrostatic repulsion at the N1−C2=O locus. Mutation of Asp 120 to an asparagine, however, would be expected to lower the pK value of the FAD hydroquinone as compared to the wild-type enzyme. In future work, pH-dependent studies of the midpoint potential will be performed, as described in ref *39*, to determine directly the proton stoichiometry of reduction for the wild-type and Asp120Asn enzymes.

Asp 120 Participates in Catalysis of the Folate Half-Reaction, Perhaps by Stabilizing the 5-Iminium Cation. On the basis of the modeling of CH_3-H_4folate into the MTHFR active site (Figure 2), we proposed roles for Asp 120 in binding of CH_2-H_4folate and in stabilization of the 5-iminium cation during catalysis. Although the model suggests bidentate hydrogen bonding between the carboxylate oxygens of Asp 120 and the N3 and 2-amino groups of the folate substrate, we have found that the apparent K_d for CH_2-H_4folate is increased only 2-fold by the Asp120Asn mutation (Figure 4, Table 1). The amide substitution in Asn 120 would have been expected to disrupt one of the hydrogen bonds. Structures of folate complexes of the wild-type and mutant enzymes may offer explanations for the failure of the Asp120Asn mutation to perturb the binding constant.

Our results demonstrate that, while the Asp120Asn mutation has a small effect on binding of CH_2-H_4folate, it has significantly decreased the ability of the enzyme to catalyze folate-dependent reactions in either direction (Tables 1 and 2). These data are consistent with a role for Asp 120 in the formation and/or stabilization of the high-energy folate intermediate, the 5-iminium cation, during catalysis. Although the existence of a 5-iminum cation has not been demonstrated directly in MTHFR, the intermediate is a reasonable first step in activation of the CH_2-H_4folate for hydride transfer from the reduced flavin (See Scheme 1). A three-step catalytic process can be envisioned to promote ring opening of CH_2-H_4folate and generation of the 5-iminium cation in MTHFR: first, the enforcing of the proper orientation of the five-membered imidazolidine ring of CH_2-H_4folate (*10*, *40*), perhaps concomitant with substrate binding; second, protonation of N10 by an acid catalyst to increase its leaving group ability (*10*); and third, electrostatic stabilization of the resulting high energy cationic intermediate. Our results with the Asp120Asn mutant MTHFR suggest that it is able to bind CH_2-H_4folate in its ring-closed form, but then is impaired in the conversion to the 5-iminium cation by one of the above steps. Structural studies of the analogous mutation (Asp169Asn) in *E. coli* thymidylate synthase lend support to a role for orientation in CH_2-H_4folate catalysis. Asp 169 hydrogen bonds to N3 and, via a water molecule, to the 2-amino group of CH_2-H_4folate (*10*). The Asp169Asn mutant enzyme catalyzes dTMP product formation 8000-

fold slower than the wild-type enzyme; it is significantly impaired in CH_2-H_4folate binding and in formation of the covalent ternary complex of enzyme, CH_2-H_4folate, and 2′-deoxyuridine 5′-monophosphate (dUMP) (*40*, *41*). The crystal structure of the inhibitory, ternary complex of Asp169Asn enzyme, CH_2-H_4folate, and FdUMP (5-fluoro-dUMP) shows CH_2-H_4folate bound at an alternate, nonproductive site on the enzyme with its imidazolidine ring closed (*40*); for comparison, the structure of the analogous wild-type enzyme complex reveals a stable structural analogue of the covalent ternary intermediate productively bound at the active site (*10*). These structures suggest that in the Asp169Asn mutant, nonproductive binding of CH_2-H_4folate has prevented imidazolidine ring opening. In contrast, the structure of a ring-opened folate analogue in a ternary complex with Asp169Asn mutant enzyme and dUMP shows the folate bound in the productive orientation for catalysis (*40*), essentially identical to its position in the corresponding wild-type enzyme complex (*10*). Taken together, the available data suggest that the Asp169Asn mutation interferes with ring opening and 5-iminium cation formation in thymidylate synthase. Future structural studies of wild-type and Asp120Asn MTHFR enzymes in complex with both ring-closed and ring-opened folate analogues may help to ascertain whether the proper orientation of the imidazolidine ring plays an important role in MTHFR catalysis. The monophasic kinetics observed for oxidation of reduced mutant enzyme by CH_2-H_4folate (Figure 4) stands in contrast to the biphasic pattern observed for the wild-type enzyme (Figure 4 in ref *1*). Until we understand the origin of the biphasic kinetics observed for the wild-type enzyme (see preceding paper in this issue for discussion) we will not be able to interpret the factors leading to the observed differences between mutant and wild-type enzyme.

Our data are consistent with a role for Asp 120 of MTHFR in electrostatic stabilization of the 5-iminium cation, once it is formed. The ionization state of the Asp 120 carboxylate side chain within MTHFR is not known. However, the observed increase in midpoint potential for the Asp120Asn mutation (Table 1) suggests that a negative charge near the flavin has been lost. If the pK_a of the Asp 120 carboxylate side chain is close to that in solution (p$K_a \approx 4$), Asp 120 would be negatively charged and able to stabilize a developing positive charge on the 5-iminium cation intermediate. From our CH_3-H_4folate docking model (Figure 2), the distance between the Asp 120 side chain and N5 of the 5-iminium folate cation is estimated to be ∼6.3 Å consistent with favorable electrostatic interactions. Simple coulombic interaction energies will be modulated by solvent shielding and the partial charges of intervening groups, but electrostatic effects could still be significant at this distance. Such relatively long-range electrostatic interactions have been proposed (Asp 27) in *E. coli* dihydrofolate reductase. Asp 27, the only ionizable group near the H_2folate substrate, is positioned 5 Å from the N5 atom and hydrogen bonds to N3 and 2-amino group of the pterin ring (*14*). The Asp27Asn mutant enzyme has a 300-fold lower catalytic activity compared to the wild-type enzyme and is deficient in the N5 protonation step needed to promote hydride transfer (*43*). Recent data suggest that the side chain of Asp 27 has a pK_a below 4 and is ionized at the active site of the enzyme (*44*). Raman difference spectroscopy has further shown that the

pK_a of the enzyme-bound N5 atom of folate is 6.5 compared with 2.6 in solution (*45*). Taken together, these data suggest that during catalysis, Asp 27 remains ionized and facilitates protonation of N5 by raising its pK_a via long-range electrostatic interactions, perhaps involving bound water molecules. We propose that an electrostatic effect similar to that in dihydrofolate reductase may allow a negatively charged Asp 120 in MTHFR to stabilize the putative 5-iminium cation intermediate.

Glu 28 Has an Essential Role in Folate Activation and/ or Catalysis. We have proposed that Glu 28 of MTHFR, located near N10 of the folate (Figure 2), may serve as a general acid catalyst involved in opening of the imidazolidine ring and generation of the 5-iminium cation required for catalysis. Our results show that the Glu28Gln mutant enzyme is defective in folate-dependent catalysis; it is unable to catalyze the reduction of CH_2-H_4folate to CH_3-H_4folate or the reverse of this reaction and is inactive in the physiological NADH-CH_2-H_4folate oxidoreductase reaction (Tables 1 and 2). For comparison, the Glu60Gln mutant of *E. coli* thymidylate synthase shows a 370-fold decrease in overall dTMP product formation (*20*) and the Glu28Gln (*46*), Glu60Ala, and Glu60Leu (*47*) mutants are greatly slowed in the formation of the covalent ternary complex between enzyme, CH_2-H_4folate, and dUMP. Although these data suggest that Glu 60 may assist in imidazolidine ring opening, the isolation by SDS/PAGE of the covalent intermediates of the Glu60Ala and Glu60Leu mutants indicates that Glu 60 it is not essential for complex formation (*47*). Interestingly, structural analysis of the Glu60Gln mutant enzyme provides evidence that Glu 60, in its ionized form, coordinates a water-mediated hydrogen bond network that promotes proton-transfer reactions at the folate and dUMP substrates (*48*). In MTHFR, the ionization state of Glu 28 is not known; direct protonation of N10 by Glu 28, acting as a general acid catalyst, would require an elevated pK_a for the carboxylic acid side chain. The observed increase in midpoint potential for the Glu28Gln mutation (Table 1); however, indicates a loss of a negative charge near the flavin and suggests that Glu 28 exists as the carboxylate anion, at least in the substrate-free state of the enzyme. Experiments examining the pH dependence of the folate-dependent oxidative half-reaction may be informative here. We hypothesize that, similar to Glu 60 of thymidylate synthase, Glu 28 of MTHFR may coordinate a hydrogen-bonding network of water molecules, which in communication with the solvent, may serve as the ultimate proton donor to the N10 atom of CH_2-H_4folate. In addition, Glu 28, in its ionized form, may play an important role in the electrostatic stabilization of the resulting 5-iminium cation, as we have suggested for Asp 120.

Glu 28 Also Participates in NADH Catalysis. Our results demonstrate that, in addition to a critical role in folate catalysis, Glu 28 is significantly involved in oxidation of the NADH substrate (Figure 6, and Tables 1 and 2). The reductive half-reaction occurs by transfer of the 4S-hydrogen of NADH as a hydride to the N5 position of the FAD (*4*). Because the transition state for hydride transfer is sensitive to the relative orientations of the NADH and FAD (*49*), the binding of NADH in a different orientation to the Glu28Gln enzyme could presumably hinder catalysis. Flavin-pyridine nucleotide charge-transfer complexes are believed to be indicators of the proper orientation for hydride transfer (*49*).

A charge-transfer complex, probably between oxidized enzyme and NADH, is observed for wild-type MTHFR (Figure 2B in ref *1*), but not for the Glu28Gln enzyme. This suggests that NADH may not be bound in the optimal orientation for hydride transfer in the mutant enzyme, accounting for its significantly decreased activity. It is interesting to note that although the relative orientation between NADH and Glu 28 has a major influence on catalysis, its effect on the K_d for NADH is minimal (Figure 6, Tables 1, 2).

In summary, modeling of CH_3-H_4folate into the structure of *E. coli* MTHFR (Figure 2) implicated two conserved amino acid residues, Asp 120 and Glu 28, as potential catalysts of the reaction with folate. In this paper, we have characterized the properties of the Asp120Asn and Glu28Gln mutant enzymes and our results support involvement of these residues in folate activation and/or catalysis. We have drawn useful parallels between the mechanisms of *E. coli* MTHFR and the structurally unrelated enzyme, thymidylate synthase. Both MTHFR and thymidylate synthase presumably catalyze activation of CH_2-H_4folate to the more reactive 5-iminium cation and both contain a glutamate and an aspartate residue in proximity to the folate at their active site. In MTHFR, the unusual aspartate residue above the N1−C2═O position of the flavin may be a requirement for activation of the folate substrate.

ACKNOWLEDGMENT

REFERENCES

1. Trimmer, E. E., Ballou, D. P., and Matthews, R. G. (2001) *Biochemistry 40*, 6205−6215.
2. Vanoni, M. A., Ballou, D. P., and Matthews, R. G. (1983) *J. Biol. Chem. 258*, 11510−11514.
3. Daubner, S. C., and Matthews, R. G. (1982) *J. Biol. Chem. 257*, 140−145.
4. Vanoni, M. A., and Matthews, R. G. (1984) *Biochemistry 23*, 5272−5279.
5. Sumner, J. S., and Matthews, R. G. (1992) *J. Am. Chem. Soc. 114*, 6949−6956.
6. Guenther, B. D., Sheppard, C. A., Tran, P., Rozen, R., Matthews, R. G., and Ludwig, M. L. (1999) *Nat. Struct. Biol. 6*, 359−365.
7. Massey, V. (1995) *FASEB J. 9*, 473−475.
8. Fraaije, M. W., and Mattevi, A. (2000) *Trends Biochem. Sci. 25*, 126−132.
9. Kallen, R. G., and Jencks, W. P. (1966) *J. Biol. Chem. 241*, 5845−5850.
10. Matthews, D. A., Villafranca, J. E., Janson, C. A., Smith, W. W., Welsh, K., and Freer, S. (1990) *J. Mol. Biol. 214*, 937−948.
11. Carreras, C. W., and Santi, D. V. (1995) *Annu. Rev. Biochem. 64*, 721−762.
12. Perry, K. M., Carreras, C. W., Chang, L. C., Santi, D. V., and Stroud, R. M. (1993) *Biochemistry 32*, 7116−7125.
13. Lee, H., Reyes, V. M., and Kraut, J. (1996) *Biochemistry 35*, 7012−7020.
14. Bystroff, C., Oatley, S. J., and Kraut, J. (1990) *Biochemistry 29*, 3263−3277.

15. Matthews, D. A., Alden, R. A., Bolin, J. T., Freer, S. T., Hamlin, R., Xuong, N., Kraut, J., Poe, M., Williams, M., and Hoogsteen, K. (1977) *Science 197*, 452−455.

16. Hampele, I. C., D'Arcy, A., Dale, G. E., Kostrewa, D., Nielsen, J., Oefner, C., Page, M. G. P., Schoenfeld, H.-J., Stueber, D., and Then, R. L. (1997) *J. Mol. Biol. 268*, 21−30.

17. Achari, A., Somers, D. O., Champness, J. N., Bryant, P. K., Rosemond, J., and Stammers, D. K. (1997) *Nat. Struct. Biol. 4*, 490−497.

18. Schmidt, A., Wu, H., MacKenzie, R. E., Chen, V. J., Bewly, J. R., Ray, J. E., Toth, J. E., and Cygler, M. (2000) *Biochemistry 39*, 6325−6335.

19. Hyatt, D. C., Maley, F., and Montfort, W. R. (1997) *Biochemistry 36*, 4585−4594.

20. Zapf, J. W., Weir, M. S., Emerick, V., Villafranca, J. E., and Dunlap, R. B. (1993) *Biochemistry 32*, 9274−9281.

21. Tabor, S., and Richardson, C. C. (1985) *Proc. Natl. Acad. Sci. U.S.A. 82*, 1074−1078.

22. Patel, P., and Ballou, D. P. (2000) *Anal. Biochem. 286*, 187−192.

23. Sheppard, C. A., Trimmer, E. E., and Matthews, R. G. (1999) *J. Bacteriol. 181*, 718−725.

24. Horton, R. M., Ho, S. N., Pullen, J. K., Hunt, H. D., Cai, Z., and Pease, L. R. (1993) *Methods. Enzymol. 217*, 270−279.

25. Whitfield, C. D., Steers, E. J., and Weissbach, H. (1970) *J. Biol. Chem. 245*, 390−401.

26. Fasman, G. D. (1976) *Handbook of Biochemistry and Molecular Biology*, Vol. I, 3rd ed., CRC Press, Inc., Cleveland, OH.

27. Clark, W. M. (1960) *Oxidation−Reduction Potentials of Organic Systems*, Williams & Wilkins, Baltimore.

28. Minnaert, K. (1965) *Biochim. Biophys. Acta 110*, 42−56.

29. Williams, C. H., Jr., Arscott, L. D., Matthews, R. G., Thorpe, C., and Wilkinson, K. D. (1979) *Methods Enzymol 62*, 185−98.

30. Massey, V. (1991) in *Flavins and Flavoproteins 1990* (Curti, B., Ronchi, S., and Zanetti, G., Eds.) pp 59−66, Walter de Gruyter, Berlin.

31. Wohlfarth, G., and Diekert, G. (1991) *Arch. Microbiol. 155*, 378−381.

32. Massey, V., Gibson, Q. H., and Veeger, C. (1960) *Biochem. J. 77*, 341−351.

33. Cleland, W. W. (1979) *Methods Enzymol. 63*, 500−513.

34. Ghisla, S., and Massey, V. (1989) *Eur. J. Biochem. 181*, 1−17.

35. Ghisla, S., and Massey, V. (1986) *Biochem. J. 239*, 1−12.

36. Sanner, C., Macheroux, P., Rüterjans, H., Müller, F., and Bacher, A. (1991) *Eur. J. Biochem. 196*, 663−672.

37. Vervoort, J., Van Berkel, W. J. H., Müller, F., and Moonen, C. T. W. (1991) *Eur. J. Biochem. 200*, 731−738.

38. Müh, U., Massey, V., and Williams, C. H., Jr. (1994) *J. Biol. Chem. 269*, 7982−7988.

39. Matthews, R. G., and Williams, C. H., Jr. (1976) *J. Biol. Chem. 251*, 3956−3964.

40. Sage, C. R., Michelitsch, M. D., Stout, T. J., Biermann, D., Nissen, R., Finer-Moore, J., and Stroud, R. M. (1998) *Biochemistry 37*, 13893−13901.

41. Chiericatti, G., and Santi, D. V. (1998) *Biochemistry 37*, 9038−9042.

42. Honig, B., and Nicholls, A. (1995) *Science 268*, 1144−1149.

43. Howell, E. E., Villafranca, J. E., Warren, M. S., Oatley, S. J., and Kraut, J. (1986) *Science 231*, 1123−1128.

44. Casarotto, M. G., Basran, J., Badii, R., Sze, K.-H., and Roberts, G. C. K. (1999) *Biochemistry 38*, 8038−8044.

45. Chen, Y.-Q., Kraut, J., Blakley, R. L., and Callender, R. (1994) *Biochemistry 33*, 7021−7026.

46. Hardy, L. W., Graves, K. L., and Nalivaika, E. (1995) *Biochemistry 34*, 8422−8432.

47. Huang, W., and Santi, D. V. (1994) *J. Biol. Chem. 269*, 31327−31329.

48. Sage, C. R., Rutenber, E. E., Stout, T. J., and Stroud, R. M. (1996) *Biochemistry 35*, 16270−16281.

49. Blankenhorn, G. (1975) *Eur. J. Biochem. 50*, 351−356.

50. Franken, H.-D., Rüterjans, H., and Müller, F. (1984) *Eur. J. Biochem. 138*, 481−489.